Surface orientational order at liquid-vapor interfaces induced by dipole–image-dipole interactions

Jae-Hie J. Cho and Bruce M. Law
Condensed Matter Laboratory, Department of Physics, Kansas State University, Manhattan, Kansas 66506-2601
(Received 11 November 2002; published 21 March 2003)

Highly dipolar molecules become orientationally ordered in the vicinity of a surface due to the electrostatic interaction with their image dipoles. We study this orientational order α_2 at the noncritical liquid-vapor interface of critical dipolar+nonpolar mixtures using ellipsometry. The dipolar molecules, which are strongly desorbed from the interface, possess an orientational order which is well described by $\alpha_2 \sim -t^{2\beta} D_{\pm}(z/\xi)$, where $t=|T-T_c|/T_c$ is the reduced temperature relative to the critical temperature T_c, $D_{\pm}$ is a universal function of the distance z and the *surface* correlation length $\xi=\xi^s_{o+}t^{-\nu}$, while $\beta=0.328$ and $\nu=0.632$ are standard critical exponents. The dipoles, which are preferentially oriented parallel to the surface, are repelled by their image dipoles, where $\xi^s_{o+}>\xi^b_{o+}$ (the bulk correlation length amplitude).

DOI: 10.1103/PhysRevE.67.031605 PACS number(s): 68.03.−g, 68.35.Md, 05.70.Np, 68.35.Rh

I. INTRODUCTION

For *AB* binary liquid mixtures, if the surface energy $\sigma_A \ll \sigma_B$, then the surface will be *completely saturated* by component *A* and the adsorption is frequently then called strong adsorption. The local volume fraction of component *A*, $v(z)$, varies with depth z into the liquid, from pure *A* at the surface ($z=0$) to its bulk value well into the liquid ($z\to\infty$) [1]. If, however, the surface energies of the two components are similar (weak adsorption) then this variation in composition must also depend upon the difference in surface energies ($\Delta\sigma=\sigma_A-\sigma_B$), i.e., $v(z,\Delta\sigma)$. This is a classic problem in surface physics or chemistry [2,3], whose solution has only recently been solved [4,5], where surprisingly, the adsorption behavior becomes simpler near the critical consolute point of the liquid mixture, primarily because $v(z,\Delta\sigma)$ is now described by a universal function of z and $\Delta\sigma$.

An additional complication that may occur under appropriate circumstances, is that molecules can become orientationally ordered at surfaces [6,7], where the orientational order $\alpha_2(z)$ (defined below) is also a function of depth. In this publication, we consider dipolar orientational order which occurs at the liquid-vapor surface of highly dipolar (D) + nonpolar (N) critical mixtures in the limit of strong adsorption ($|\Delta\sigma|$ large). A qualitative understanding of the dipolar behavior can be obtained by considering a dipole interacting with its image dipole in the vicinity of a surface. For a dipole in phase α, of dipole moment p at depth z and angle θ with respect to the $\hat{z}$ axis, the interaction energy with its image dipole in phase v is given by [8,9]

$$U=+\frac{kp^2(\varepsilon_\alpha-\varepsilon_v)(\cos^2\theta+1)}{16\varepsilon_\alpha(\varepsilon_\alpha+\varepsilon_v)z^3}, \tag{1}$$

where $\varepsilon_\alpha \equiv \varepsilon_\alpha(0)$ and $\varepsilon_v \equiv \varepsilon_v(0)$ are the static permittivities in the α and v phases, respectively, and $k=1/4\pi\varepsilon_o \simeq 9\times10^9$ Nm^2/C^2 in MKS units, where ε_o is the dielectric permittivity. Two types of dipolar orientational order can occur depending upon whether (*A*) $\varepsilon_\alpha<\varepsilon_v$ or (*B*) $\varepsilon_\alpha>\varepsilon_v$. For condition *A* (*B*), (i) the dipoles in the α phase, sufficiently close to the interface, lie preferentially perpendicular (parallel) to the interface with $\theta=0$ or π ($\theta=\pi/2$ or $3\pi/2$) in order to minimize the energy; (ii) as the energy is negative (positive) the dipoles are attracted to (repelled from) the surface in order to further minimize the energy; (iii) large dipole moments p give rise to large orientational ordering effects; and (iv) the orientational order must vanish in the bulk liquid phase ($z\to\infty$).

Conditions (i)–(iv) provide a qualitative understanding of the dipolar behavior due to the long-range electrostatic interaction. Short-range interactions also play an important role in determining the surface behavior. For a dipolar+nonpolar critical mixture the surface energies (or surface tensions) determine the short-range behavior. If (a) $\sigma_D<\sigma_N$ then component *D* is preferentially adsorbed at the surface while for (b) $\sigma_D>\sigma_N$, the converse occurs. Thus, conditions *A* and *B* when combined with conditions a and b lead to four classes of behavior. In class Aa both the long- and short-range forces attract the dipole to the surface, where the dipole is oriented preferentially perpendicular to the surface. In class Bb, the long- and short-range forces repel the dipole from the surface, where the dipole is preferentially oriented parallel to the surface. Finally, in classes Ab and Ba the short- and long-range interactions oppose each other, where one is attractive and the other is repulsive.

In a previous paper [10], we described two *DN* critical mixtures whose one-phase surface orientational order behavior fell within class Bb. In this publication we expand upon this earlier work but also consider the more complicated two-phase region. In order to understand dipole surface orientational order, strong critical adsorption in the absence of orientational order is first described in Sec. II. Various models for surface orientational order are considered in Sec. III. Experimental details are provided in Sec. IV while the experimental results are compared with the models from Secs. II and III in Sec V. The main results from this paper are summarized and discussed in Sec. VI. The analysis which connects the local volume fraction of the adsorbed component $v(z)$, surface orientational order $\alpha_2(z)$, and optical signal is rather complex. A summary of this optical calculation is therefore provided in the Appendix (Sec. VII).

TABLE I. Strong adsorption model parameters.

Phase	$x_{o\pm}$	$c_{\pm}$	$c_{1\pm}$	$c_{2\pm}$	$P_{\infty\pm}$	$P_{1\pm}$	$P_{2\pm}$
1	1.57	0.792	−0.286	0.033	0.826	3.266	−4.394
2	0.86	1.123	0.148	0.0051	0.659	−0.515	2.076

II. UNIVERSAL SCALING FUNCTION FOR STRONG CRITICAL ADSORPTION

In the absence of orientational ordering effects, the surface is locally isotropic and the local order parameter $m(z)$ is defined by [1,3]

$$m(z)=v(z)-v_c \tag{2}$$

$$=M_- t^{\beta} P_{\pm}[(z+z_e)/\xi_{\pm}], \tag{3}$$

where the second line follows from scaling theory for critical liquid mixtures in the strong critical adsorption limit (which is valid provided that the surface energy difference between the two liquid component $|\Delta\sigma| \gtrsim 6$ erg/cm^2 for room temperature critical mixtures [11]). Here v_c is the critical volume fraction, $t=|T_c-T|/T_c$ is the reduced temperature relative to the critical temperature T_c, $M_- t^{\beta}$ describes the shape of the coexistence curve, the correlation length $\xi_{\pm}=\xi_{o\pm} t^{-\nu}$, the standard critical exponents $\beta=0.328$ and $\nu=0.632$, $P_{\pm} \equiv P_{\pm}(x)$ is a universal surface scaling function, while the subscript + (−) refers to quantities in the one (two)-phase region. For strong critical adsorption, $P_{\pm}$ is well described by [12]

$$P_{\pm}(x) = \begin{cases} c_{\pm} x^{-\beta/\nu} + c_{1\pm} x^{(1-\beta)/\nu} + c_{2\pm} x^{(2-\beta)/\nu}, & x \leqslant x_{o\pm} \\ P_{\pm}(\infty) + P_{\infty\pm} e^{-x} + P_{1\pm} e^{-2x} + P_{2\pm} e^{-3x}, & x > x_{o\pm}, \end{cases} \tag{4}$$

where $P_+(\infty)=0$ and $P_-(\infty)=1$ ensure that the bulk behavior at $z\to\infty$ is correct, the fourteen parameters $c_{\pm}$, $c_{1\pm}$, $c_{2\pm}$, $P_{\infty\pm}$, $P_{1\pm}$, $P_{2\pm}$, and $x_{o\pm}$ are listed in Table I [13], the extrapolation length that appears in Eq. (3)

$$z_e \simeq \xi_{o\pm} \left(\frac{1-v_c}{M_- c_{\pm}} \right)^{-\nu/\beta} \tag{5}$$

limits the volume fraction at the surface ($z=0$) to its saturated value [$v(0)=1$], while the universal correlation length amplitude [14]

$$\xi_{o+}/\xi_{o-} \equiv R_{\xi} (\simeq 1.96). \tag{6}$$

This form for $P_{\pm}$ (i) conforms with theoretical expectations at small [1] and large x [16], (ii) is continuous at T_c (as required because the system is second order), (iii) is continuous up to and including the third derivative with respect to x, and (iv) provides an excellent quantitative description of the critical adsorption behavior for five nonpolar [11] or weakly dipolar [15,12] critical binary liquid mixtures. Other forms for $P_{\pm}$ have also been considered [12]; all forms for $P_{\pm}$ are essentially identical when plotted as a function of x, hence, Eq. (4) is sufficient for our purpose. In summary, the local volume fraction $v(z)$ for any strongly adsorbing critical mixture is completely determined, according to Eqs. (2)–(6), once the system dependent parameters v_c, T_c, M_-, and ξ_{o+} are known.

III. SURFACE ORIENTATIONAL ORDER

For critical binary liquid mixtures composed of a nonpolar and a highly dipolar component, the local volume fraction of both components will vary with depth (as discussed in the preceding section), but additionally, the orientational order of the dipolar component will also vary with depth because of its interaction with its image dipole when in the vicinity of an interface [Eq. (1)]. Hence, one must define a generalized volume fraction $v(z,\theta)$ with dipole orientation θ relative to the $\hat{z}$ axis, where it is convenient to use the following decomposed [9]:

$$v(z,\theta)=\overline{v}(z)\,\alpha(z,\theta). \tag{7}$$

Here $\overline{v}(z)$ is an angle averaged volume fraction over θ and $\alpha(z,\theta)$ is a dimensionless orientational order parameter that satisfies the normalization condition

$$\int_0^{\pi} \alpha(z,\theta) \sin\theta \, d\theta = 1. \tag{8}$$

We assume that the function $\overline{v}(z)$ is identical to $v(z)$ for strong critical adsorption. Following [9], the angular dependence of $\alpha(z,\theta)$ can be expressed in terms of Legendre's polynomials $P_l(\cos\theta)$,

$$\alpha(z,\theta)=\sum_0^{\infty} \alpha_l(z) P_l(\cos\theta) \simeq \frac{1}{2} + \alpha_2(z) \frac{(3\cos^2\theta - 1)}{2}, \tag{9}$$

for dipolar molecules in the absence of any external fields [whence, $\alpha_l(z)=0$ for l odd]. The orientational order, at the liquid-vapor surface, is therefore completely described by the orientational order parameter $\alpha_2(z)$ which is negative (positive) when the dipoles are parallel (perpendicular) to the interface [9] where, in addition, the orientational order must vanish in the bulk phase [$\alpha_2(\infty)=0$]. For an isotropic interface, $\alpha_2(z)=0$ for all z.

Although the variation in the orientational order of dipolar molecules as a function of depth has been considered extensively in numerous theories and computer simulations [9,17–20], there have been very few experimental measurements of this quantity. Normally, the average orientation within a monolayer has been measured [21] without much concern as to how the orientation varies with depth away from the surface. There are a few exceptions. The orientation, and in some cases layering, has been considered for liquid crystals

approaching their isotropic-nematic [22] or isotropic-smectic [23] phase transition points, however, the surface orientational order is driven in this case by a different mechanism than considered here. For dipole–induced-dipole orientation at surfaces, Teixeira *et al.* [24] measured and compared the change in surface tension for varying dipole volume fraction in binary liquid mixtures with theoretical calculations, while Yang *et al.* [20] compared a variety of experimental measurements for the orientation of water at the liquid-vapor interface with theoretical calculations. In both of these studies, the experiments measured an integral over $\alpha_2(z)$ rather than $\alpha_2(z)$ directly.

There are two principal difficulties in measuring $\alpha_2(z)$ at the surfaces of binary liquid mixtures: (i) both $\alpha_2(z)$ and $v(z)$ vary with z, therefore, it is only possible to determine $\alpha_2(z)$ once $v(z)$ is quantitatively understood and (ii) neither $\alpha_2(z)$ nor $v(z)$ are measured directly. They can only be inferred by considering how these quantities alter the optical properties of light reflected from a structured surface. This is a complicated problem usually involving a numerical solution of Maxwell's equation, while taking into account the local surface structure.

In prior work [25,26], the orientational order was considered at the *critical* liquid-liquid interface of critical dipolar + nonpolar binary liquid mixtures, where the system phase separated into a dipole-rich and a dipole-poor phases. Theory had previously suggested that [17,9]

$$\alpha_2(z) \sim d^2 m(z)/dz^2 \tag{10}$$

$$\sim t^{\beta+2\nu} X(z/\xi), \tag{11}$$

where $m(z)$ corresponds to the variation in the local order parameter through a *critical* interface and $X(z/\xi)$ is a universal function of z/ξ. The form for $m(z)$ is well known [27], thus, Eq. (10) could be quantitatively tested. Indeed, this equation provided a quantitative description of experimental optical data for two highly dipolar+nonpolar critical mixtures [25,26] with known dipole moment. It also provided qualitative support for the presence of orientational order at the critical interface of a critical ionic solution [28]. The form of $\alpha_2(z)$ implies that the dipoles preferentially orient parallel (perpendicular) to the interface in the dipole-rich (dipole-poor) phase, in agreement with both density functional calculations [9] and the simple electrostatic considerations of Eq. (1). However, Eq. (10) cannot be predicted via considerations of Eq. (1); instead, Eq. (10) arises via functional minimization of the total free energy with respect to the orientational order and composition through the interface [17].

Could Eq. (10) also describe the orientational order that occurs at the *noncritical* liquid-vapor interface, where now $m(z)$ represents the local order parameter for strong critical adsorption [Eqs. (3) and (4)]? Later considerations in Sec. V indicate that Eq. (10) cannot describe the behavior at this interface and therefore, it is necessary to discuss more general forms that $\alpha_2(z)$ might take. Following analogous theoretical considerations to [1], $\alpha_2(z)$ is expected to take the form

$$\alpha_2(z) \sim t^{\phi} Y_{\pm}[(z+z_e)/\xi], \tag{12}$$

where ϕ is a new critical exponent and $Y_{\pm}(x)$ is a universal surface scaling function with

$$Y_{\pm}(x) \sim \begin{cases} x^{-\phi/\nu}, & x \ll 1 \\ e^{-x}, & x \gg 1. \end{cases} \tag{13}$$

The small x behavior ensures that $\alpha_2(z)$ is finite and nonzero at the critical temperature T_c (using analogous arguments to Ref. [1]), while the large x behavior is expected according to Ref. [16]. A simple algebraic crossover function of the form

$$\alpha_2(x) = c'_{o\pm} t^{\phi} \left(\frac{1 + c'_{\pm} x}{x} \right)^{\phi/\nu} e^{-x} \tag{14}$$

should be sufficient to describe Eq. (13) [16] where, for continuity at T_c, we require that

$$c'_{o+}/c'_{o-} = R_{\xi}^{-\phi/\nu}. \tag{15}$$

Hence, according to Eqs. (14) and (15), there are five adjustable parameters, namely, c'_{o-}, $c'_{\pm}$, ϕ, and ξ_{o+} (if ξ_{o+} differs from its bulk value—see later) with which to improve the agreement between theory and experiment. Additionally, the electrostatics consideration of Eq. (1) imply that c'_{o+} is negative for the liquid-vapor surface [i.e., the dipoles are oriented primarily parallel to the interface on the "liquid side" of the interface $(z>0)$].

After tedious calculations adjusting these five parameters, the optimal solution seems to be when $\phi \simeq 2\beta$ (Sec. V), which is at variance with the result found at the *critical* interface [Eq. (11)]. If one continues to believe that the local orientational order $\alpha_2(z)$ is related to a function of the local order parameter $m(z)$, as proposed by theory [29], then the result $\phi \simeq 2\beta$ suggests that perhaps

$$\alpha_2(z) \sim [m(z)]^2. \tag{16}$$

However, one must be careful that all of the conditions required for orientational order are fullfilled. Therefore, although Eq. (16) could potentially be valid in the one-phase regime, more care must be taken when considering the two-phase regime. This is because, in the two-phase regime, the orientational order vanishes in the bulk, $\alpha_2(\infty)=0$, whereas the order parameter is finite and nonzero in the bulk $[P_-(\infty)=1]$. A form for $\alpha_2(z)$ that obeys Eqs. (12)–(16) is

$$\alpha_2(z) = M_D [t^{\beta} D_{\pm}(x)]^2, \tag{17}$$

where

$$D_+(x)=P_+(x), \quad D_-(x)=c_-\left(\frac{1+d_-x}{x}\right)^{\beta/\nu}e^{-x}, \quad (18)$$

c_- is given in Table I, while M_D and d_- are adjustable constants. The structure of D_- is very similar to the structure of P_-, to leading order, except that D_- approaches 0 (rather than 1) in the bulk. The various forms for $\alpha_2(x)$, discussed in this section, will be compared with experimental data in Sec. V.

IV. EXPERIMENTAL DETAILS

A. Sample preparation and sample parameters

Dipole orientational order is expected to be present at surfaces when the reduced dipole moment [9]

$$p^*=p/\sqrt{\delta^3 u_0}\gtrsim 2, \quad (19)$$

where δ is the average hard sphere diameter and u_0 is the Lennard-Jones potential well depth. Two highly dipolar + nonpolar critical mixtures are considered in this publication. The heavier dipolar component was either 2-nitroanisole (2N) or 4-nitroanisole (4N), where both liquids have a large dipole moment $p(\sim 5D)$ with reduced dipole moment $p^*\sim 2$ (Table III), while the lighter nonpolar component was cyclohexane (C). The 2-nitroanisole and cyclohexane, with purity of 99+%, were purchased from Aldrich and used without any further purification. The 4-nitroanisole, of purity 97%, was fractionally distilled to improve its transparency after purchase from Lancaster.

For both critical mixtures, a 0.5 μm teflon Millipore filter was used to remove any particulates. The sample cell consisted of a chemically resistant Pyrex cylinder of diameter ~2.3 cm and length ~7 cm. This sample cell was glass etched using a solution consisting of 60% distilled water, 35% HNO_3, and 5% HF by volume, rinsed well with double distilled deionized water before drying and half filling with a critical mixture. The critical composition v_c was found using the standard method of determining that volume fraction for which the upper and lower phases had equal volumes a few mK into the two-phase region. This cylindrical sample cell was situated horizontally inside a two-stage oven composed of an electrically heated inner stage and a water-cooled outer stage, where the temperature difference between stages was kept at approximately 6 K. Thermal gradients along the sample cell were less than ~1 mK/cm, where the thermal stability was ~1 mK per day. The critical temperatures for the mixtures were measured *in situ* by observing the spinodal ring, which appears during spinoidal decomposition; this enabled T_c to be determined within ~1 mK. At each temperature, 4 h elapsed to ensure thermal and diffusive equilibrium (the thermal time constant of the oven is actually only ~10 min.) and then ten ellipsometric ($\overline{\rho}$, see Sec. IV B) and T measurements were collected over the succeeding hour. Thus, the results presented in this paper are the average of these ten measurements. The temperature was always decreased in successive measurements so that gravity assisted in the phase separation process. The amplitude of the coexistence curve, M_-, was determined by measuring the separation temperature for a number of different noncritical samples, while the amplitude of the correlation length ξ^b_{o+} was determined either from a turbidity measurement following the procedure in Ref. [30] or by studying the critical liquid-liquid interface using ellipsometry [see Eq. (31)]; the superscript b on ξ^b_{o+} distinguishes it from the "surface" correlation length amplitude ξ^s_{o+} discussed in Sec. V. The sample parameters v_c, T_c, M_-, and ξ^b_{o+} for each mixture are listed in Table II.

TABLE II. Critical mixture parameters.

Mixtures	v_c	T_c(°C)	M_-	ξ_{nc} (nm)	ξ^b_{o+} (nm)	ξ^s_{o+} (nm)	M_D	d_-
2NC	0.6658	71.709	0.841	0.12	0.24	0.42	−15.1	0.5
4NC	0.6274	58.416	0.759	0.14	0.26	0.35	−6.2	0.5

B. Ellipsometry

In the study of surface phenomena, phase modulated ellipsometry has proven to be extremely useful [31,32]. The construction and operation of our ellipsometer, used in this study, is similar to the description and operation in Ref. [33]. A HeNe laser with wavelength $\lambda=632.8$ nm is used as the light source. After appropriate polarization and phase modulation, the reflected beam from the liquid-vapor surface, which passes normally through the sample cell walls, provides a measurement of the ellipticity,

$$\overline{\rho}\equiv \mathrm{Im}(r_p/r_s)|_{\theta_B}, \quad (20)$$

at the Brewster angle (θ_B), where r_p and r_s are the complex reflection amplitudes for polarizations parallel (p) and perpendicular (s) to the plane of incidence. The Brewster angle is operationally determined by that angle of incidence where

$$\mathrm{Re}(r_p/r_s)|_{\theta_B}=0. \quad (21)$$

The experimental $\overline{\rho}$ data, in the one- (circles) and two-phase (squares) regions at various temperatures, are exhibited in Figs. 1(a) and 1(b) for 2NC and 4NC, respectively, and is available in Ref. [34] or upon request.

For surface layers that are sufficiently thin, compared with the wavelength of light λ, namely, $\xi/\lambda\ll 1$, which occurs sufficiently far from T_c (say, $t\gtrsim 5\times 10^{-3}$ [35]), the following modified Drude's equation provides an accurate description of the ellipticity for a locally anisotropic interface [36,37]

$$\overline{\rho}\simeq \frac{\pi}{\lambda}\frac{\sqrt{\varepsilon_v+\varepsilon_l}}{\varepsilon_v-\varepsilon_l}\int_{-\infty}^{\infty}\left[\varepsilon_{\parallel}(z)+\frac{\varepsilon_v\varepsilon_l}{\varepsilon_{\perp}(z)}-(\varepsilon_v+\varepsilon_l)\right]dz. \quad (22)$$

Here ε_v (ε_l) represents the optical dielectric constant in the vapor (liquid) phase, while $\varepsilon_{\parallel}(z)$ [$\varepsilon_{\perp}(z)$] describe the local optical dielectric constant parallel (perpendicular) to the in-

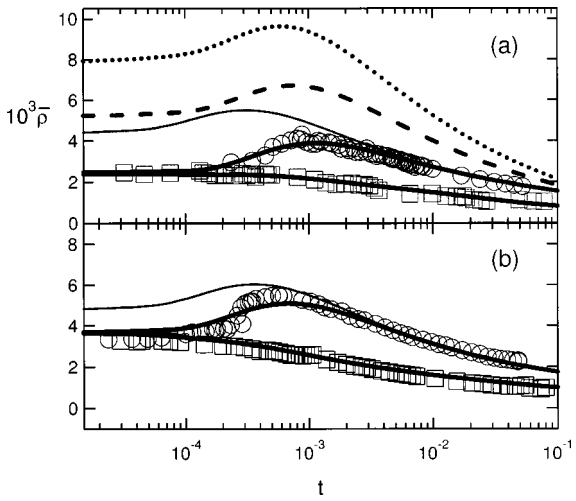

FIG. 1. (a) Comparison of various adsorption or orientational order models with the highly dipolar critical mixture 2NC in the one (circles) and two-phase (squares) regions: $\overline{\rho_P}$ model with $\xi^b_{o+}=0.24$ nm (light solid line) or $\xi^s_{o+}=0.42$ nm (dashed line) and $\overline{\rho_\alpha}$ model [Eq. (17)] with ξ^s_{o+} and $M_D=-15.1$ (heavy solid line) or $M_D=15.1$ (dotted line). For clarity, the two-phase calculation has only been shown for the best fit (heavy solid line). (b) Similar comparison for the highly dipolar mixture 4NC, where the symbols and lines have the same meaning as in (a) but with $\xi^b_{o+}=0.26$ nm, $\xi^s_{o+}=0.35$ nm, and $M_D=-6.2$.

terface at depth z. This Drude's approximation has only been used in the preanalysis of our data. For interfaces of any thickness, the ellipticity $\overline{\rho}$ can be determined by numerically solving Maxwell's equations ([38–41]) for a given model of $\varepsilon_\parallel(z)$ and $\varepsilon_\perp(z)$ as described in the Appendix. The interrelationship between $\varepsilon_\parallel(z)$ and $\varepsilon_\perp(z)$ with the local volume fraction $v(z)$ and local orientational order $\alpha_2(z)$ are discussed in the following section.

C. Anisotropic optical dielectric constant at the interface

Most molecules which possess a permanent dipole moment are nonspherical in shape and have an anisotropic optical polarizability [42] represented by the dipole's optical dielectric ellipsoid $(\varepsilon_1,\varepsilon_2,\varepsilon_3)$, where the ε_1 axis is choosen to point along the dipole moment p direction, while ε_2 (ε_3) is choosen to point in the plane (perpendicular to the plane) of the benzene ring for the nitroanisole molecule. Near an interface, if the dipole becomes orientationally ordered then the local dielectric constant at depth z will be anisotropic, with differing values parallel $[\varepsilon_\parallel(z)]$ and perpendicular $[\varepsilon_\perp(z)]$ to the interface. This local optical dielectric anisotropy influences the ellipticity of light reflected from this interface. We expect $\varepsilon_\parallel(z)$ and $\varepsilon_\perp(z)$ are related to the dielectric ellipsoid $(\varepsilon_1,\varepsilon_2,\varepsilon_3)$, the orientational order parameter $\alpha(z,\theta)$ [Eq. (9)], and the local dipolar volume fraction $v(z)$ [Eqs. (2) and (3)] through the interface.

Before discussing the optical dielectric properties within a dipolar plus nonpolar mixture [i.e., $\varepsilon_\parallel(z)$ and $\varepsilon_\perp(z)$], we first consider the optical dielectric properties of an *oriented dipole*, where a superscript *d* refers to a *dipolar* property. For a dipole oriented at angle θ to the z axis, the parallel and perpendicular components of the dipole's dielectric constant are given, respectively, by [26]

$$\varepsilon^d_\perp(\theta)=\frac{1}{\sqrt{\left(\frac{\cos^2\theta}{\varepsilon_1}+\frac{\sin^2\theta}{\varepsilon_2}\right)\left(\frac{\cos^2\theta}{\varepsilon_1}+\frac{\sin^2\theta}{\varepsilon_3}\right)}}, \quad (23)$$

and

$$\varepsilon^d_\parallel(\theta)={}_2F_1\sqrt[4]{\frac{\varepsilon_2\varepsilon_3}{\left(\frac{\sin^2\theta}{\varepsilon_1}+\frac{\cos^2\theta}{\varepsilon_2}\right)\left(\frac{\sin^2\theta}{\varepsilon_1}+\frac{\cos^2\theta}{\varepsilon_3}\right)}}. \quad (24)$$

where ${}_2F_1\equiv{}_2F_1(1/2,1/2,1;(\varepsilon_3-\varepsilon_2)/4\sqrt{\varepsilon_2\varepsilon_3})(\approx 0.98)$ is a hypogeometric function. At a particular depth z, the orientational order parameter $\alpha(z,\theta)$ describes the distribution in orientations, therefore, the angle-averaged *dipole* dielectric constants parallel $[\varepsilon^d_\parallel(z)]$ and perpendicular $[\varepsilon^d_\perp(z)]$ to the interface can be calculated from

$$\varepsilon^d_{\parallel(\perp)}(z)=\int_0^\pi \varepsilon^d_{\parallel(\perp)}(\theta)\,\alpha(z,\theta)\sin\theta\,d\theta. \quad (25)$$

For randomly oriented dipoles, where $\alpha(z,\theta)=\frac{1}{2}$ the average optical dielectric constant should correspond to the bulk dielectric constant of the dipolar component, namely,

$$\varepsilon_D=\frac{1}{2}\int_0^\pi \varepsilon^d_{\parallel(\perp)}(\theta)\sin\theta\,d\theta. \quad (26)$$

Thus, from Eqs. (9) and (26), Eq. (25) can be rewritten as

$$\varepsilon^d_{\parallel(\perp)}(z)=\varepsilon_D+\alpha_{\parallel(\perp)}\alpha_2(z), \quad (27)$$

where the anisotropy

$$\alpha_{\parallel(\perp)}=\frac{1}{2}\int_0^\pi \varepsilon^d_{\parallel(\perp)}(\theta)(3\cos^2\theta-1)\sin\theta\,d\theta. \quad (28)$$

Equation (27) is an important simplification that allows one to calculate the *dipole* optical dielectric constant parallel and perpendicular to the interfaces $[\varepsilon^d_{\parallel(\perp)}(z)]$, for any orientational order parameter $\alpha_2(z)$, once ε_D and $\alpha_{\parallel(\perp)}$ are known. The optical dielectric ellipsoid $(\varepsilon_1,\varepsilon_2,\varepsilon_3)$, dipolar optical dielectric constant ε_D, and optical anisotropy $\alpha_{\parallel(\perp)}$ [calculated from Eqs. (23), (24), and (28)], for 2-nitroanisole and 4-nitroanisole, are listed in Table III.

For binary liquid mixtures, the local volume fraction of the preferrentially adsorbed component $v(z)$ and of the dipoles vary with depth. The parallel $[\varepsilon_\parallel(z)]$ and perpendicular $[\varepsilon_\perp(z)]$ dielectric constants through the interface for a

TABLE III. Liquid parameters. (Superscript numbers represent the corresponding temperature in °C.)

Parameters	2-Nitroanisole	4-Nitroanisole	Cyclohexane
σ(erg/cm^2)[60]	41.51	42.40	20.49
ε_D or ε_N	2.339[70]	2.435[60]	1.945[70]
ε_S	34.71[70]	27.31[60]	1.945[70]
δ(nm)	0.650	0.667	
$10^{21}u_0$(J)	2.686	2.513	
$p(D)$	4.81,[a] 4.78[b]	4.75,[a] 5.22[b]	
p^*	1.77,[a] 1.76[b]	1.74,[a] 1.91[b]	
g	1.1	0.8	
$\alpha_\parallel$	−0.126	−0.156	
$\alpha_\perp$	0.256	0.315	
ε_1	3.17[c]	3.46	
ε_2	2.64	2.58	
ε_3	1.73	1.81	

[a]Reference [48].
[b]Reference [49].
[c]Reference [26].

solution can now be calculated using the two-component Clausius-Mossotti relation [43]

$$F[\varepsilon_{\parallel(\perp)}(z)]=[1-v(z)]F[\varepsilon^d_{\parallel(\perp)}(z)]+v(z)F(\varepsilon_N), \tag{29}$$

where $F(x)=(x-1)/(x+2)$ and ε_N is the optical dielectric constant of the nonpolar component (i.e., cyclohexane in this particular paper). In summary, for a particular model of $v(z)$ and $\alpha_2(z)$ on the liquid side of the interface ($z>0$), the optical dielectric constants through the interface [$\varepsilon_\parallel(z)$ and $\varepsilon_\perp(z)$] can be calculated from Eqs. (27) and (29) using data from Table III.

On the vapor side of this interface ($z<0$), dipolar molecules are absent [$\alpha_2(z)=0$] because they are desorbed from the surface. Hence, to ensure continuity of the optical dielectric constant at $z=0$ we assume that [35]

$$\varepsilon(z)=1+\frac{[\varepsilon(0)-1][1+e^{-z_e/\xi_{nc}}]}{1+e^{-(z+z_e)/\xi_{nc}}}, \quad z<0 \tag{30}$$

on the vapor side of the interface, where the extrapolation length z_e is given in Eq. (5) and ξ_{nc} (~0.13 nm for our samples) is a noncritical correlation length, which can be determined from the background ellipticity at large reduced temperatures.

V. EXPERIMENTAL RESULTS

We are now in a position to compare various theoretical models for the orientational order parameter $\alpha_2(z)$ with experimental ellipticity $\overline{\rho}$ data. Equations (29) and (30) determine the optical dielectric function from which the ellipticity $\overline{\rho}$ can be calculated using the information in the Appendix.

In the absence of orientation order when $\alpha_2(z)=0$, the calculation of the ellipticity (denoted $\overline{\rho}_P$ for strong critical adsorption) is well defined. For a particular critical mixture, once the system dependent parameters v_c, T_c, M_-, ξ^b_{o+} (Table II) and optical dielectric constants (Table III) are known, the local volume fraction $v(z)$ of the adsorbed component (cyclohexane) is completely determined by Eqs. (2)–(6), where the parameters for the $P_\pm$ model are listed in Table I. The local dielectric constant $\varepsilon(z)$ can then be calculated from the Clausius-Mossotti equation [Eq. (29)], from which the ellipticity $\overline{\rho}_P$ can be determined. Only the noncritical correlation length ξ_{nc} [Eq. (30)] is available with which to improve agreement between these calculations and experimental data; however, ξ_{nc} merely shifts the $\overline{\rho}_P$ curves vertically by a constant amount [35], for all t, and cannot change the shape of the curve. The light solid curve in Fig. 1(a) shows a comparison between $\overline{\rho}_P$ and the 2NC experimental data in the one- (open circles) and two-phase (open squares) regions. There are two important differences between $\overline{\rho}_P$ and the $\overline{\rho}$ data. Specifically, (i) the peak for the $\overline{\rho}_P$ curve, in the one-phase region, occurs at smaller t than the experimental data and (ii) the $\overline{\rho}_P$ curve possesses a larger amplitude $\Delta\overline{\rho}=\overline{\rho}_{\rm peak}-\overline{\rho}_{BG}$, where $\overline{\rho}_{\rm peak}$ ($\overline{\rho}_{BG}$) is the peak (background) value. These differences can only be due to the large dipole moment of the 2NC mixture, compared with earlier samples [12,11], because the samples are similar in all other respects.

In calculating $\overline{\rho}_P$ it is important to use reliable values for the correlation length amplitude ξ^b_{o+}. We have used turbidity [30] and a measurement of $\overline{\rho}$ at the *critical liquid-liquid surface* [26], where

$$\overline{\rho}_{l/l}\sim\xi^b_{o+}t^{\beta-\nu}/R_\xi \tag{31}$$

sufficiently close to T_c, to estimate ξ^b_{o+}. Both methods give similar values for ξ^b_{o+} (Table IV). In prior work on strong critical adsorption in nonpolar [11] or weakly dipolar mixtures [12], it was found that if $\overline{\rho}$ was plotted as a function of ξ_+ (rather than t) then the peak position always occurred at the same universal position described by [12]

$$(\xi_+/\lambda)_{peak}=\xi_{o+}t^{-\nu}_{peak}/\lambda=0.064\pm0.006, \tag{32}$$

where $t_{\rm peak}$ is the reduced temperature at the peak. However, if this equation is used to estimate ξ_{o+}, (which we will denote by ξ^s_{o+} with superscript s for surface), then ξ^s_{o+} (Table IV) is anomalously large (by a factor of ~50%) compared with ξ^b_{o+} determined from the turbidity and critical interface measurement. If Eq. (32) continues to provide a measure of the "surface" correlation length, then these re-

TABLE IV. ξ_{o+} comparision.

	ξ^b_{o+} (nm)		ξ^s_{o+} (nm)	
Mixtures	Turbidity	Eq. (31)	Eq. (32)	Eq. (17)
2NC	0.27±0.02	0.24±0.02	0.45±0.03	0.42
4NC		0.26±0.02	0.35±0.02	0.35

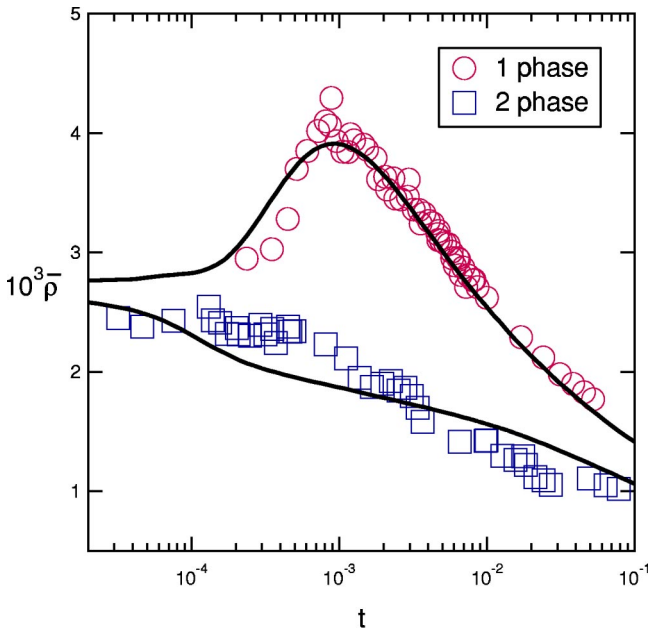

FIG. 2. Comparison of the 2NC $\overline{\rho}$ data (symbols) with the $\overline{\rho}_\alpha$ model of Eq. (14) with $c'_{o+}=-6.0$, $c'_{+}=0.8$, $c'_{-}=0.1$, $\phi=0.55$, and $\xi^s_{o+}=0.48$ nm.

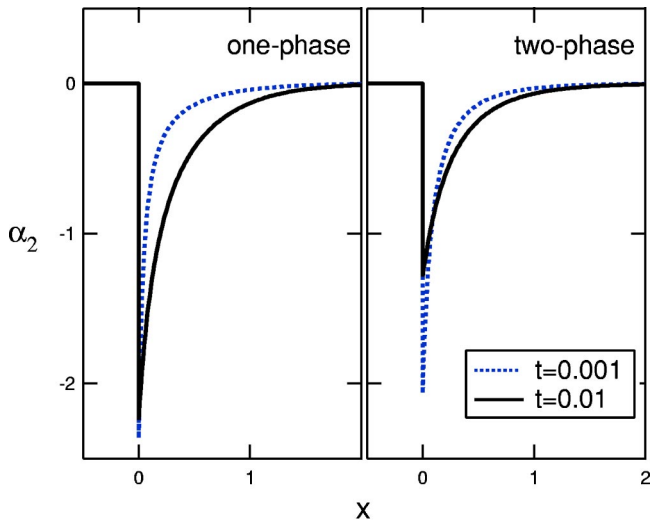

FIG. 3. Orientational order α_2 versus $x=(z+z_e)/\xi$ calculated for 2NC at two reduced temperatures t, for the one- and two-phase regions.

sults suggest that the adsorption layer is considerably thicker than what one would expect from bulk critical fluctuations. We return to this point later in this section.

The difference between $\overline{\rho}_P$ and the experimental $\overline{\rho}$ data is suspected to be due to the presence of dipole induced surface orientational order. Various models for the orientational order $\alpha_2(z)$ were discussed in Sec. III. The local parameters $v(z)$ and $\alpha_2(z)$ give rise to local optical dielectric constants parallel $[\varepsilon_\parallel(z)]$ and perpendicular $[\varepsilon_\perp(z)]$ to the interface, which can be calculated from Eqs. (27) and (29) on the liquid side of the interface $(z>0)$ using information in Table III, while on the vapor side of the interface $(z<0)$ the optical dielectric constant is governed by Eq. (30). Hence the ellipticity, which is now denoted $\overline{\rho}_\alpha$, can be determined from this optical dielectric function and the information in the Appendix. The most general expression for $\alpha_2(z)$ is given in Eq. (14), where there are five parameters c'_{o+}, $c'_{\pm}$, ϕ, and ξ_{o+} that one can adjust. In this calculation, in order to get approximate agreement with the peak $\overline{\rho}$ position, it was always necessary to increase ξ_{o+} above its bulk value as suggested earlier from considerations of Eq. (32). In Fig. 2 we show the best agreement that we could find for $\overline{\rho}_\alpha$ using this particular form for $\alpha_2(z)$. The agreement is only fair as there are noticeable deviations between $\overline{\rho}_\alpha$ and experimental data. This calculation, however, provides a hint as to how one might proceed. The best fit occurred for $\phi\simeq 2\beta$, in marked disagreement with $\phi=\beta+2\nu$ [Eq. (11)] found for dipole induced orientational order at the critical liquid-liquid interface. If we assume that (i) $\phi=2\beta$ and (ii) $\alpha_2(z)$ is related to a function of $m(z)$, then, the most obvious relationship is $\alpha_2(z)\sim[m(z)]^2$ [Eq. (16)] from which we were led to Eqs. (17) and (18). In this model for $\alpha_2(z)$ there are three adjustable parameters, ξ_{o+}, M_D, and d_-. The reduced temperature $t_{\rm peak}$ at which the $\overline{\rho}$ peak occurs is primarily controlled by ξ_{o+} and only marginally influenced by the value of M_D. This can be seen by examining Fig. 1(a). As ξ_{o+} increases from its bulk value $\xi^b_{o+}=0.24$ nm (light solid line) to the "surface" value $\xi^s_{o+}=0.42$ nm (dashed line), in the absence of orientational order (i.e., for $\overline{\rho}_P$, where $M_D=0$), then $t_{\rm peak}$ increases. However, for ξ_{o+} fixed at it's surface value ξ^s_{o+}, the position of $t_{\rm peak}$ changes only marginally for $M_D=+15.1$ (dotted line) or $M_D=-15.1$ (heavy solid line) relative to $M_D=0$ (dashed line). Another influence of increasing ξ_{o+} is that the amplitude of the ellipticity $\Delta\overline{\rho}$ also increases. The parameter M_D has a significant impact on $\Delta\overline{\rho}$; for $M_D>0(<0)$ the amplitude $\Delta\overline{\rho}$ increases (decreases)—compare the dotted, heavy solid, and dashed lines in Fig. 1(a). Finally, the parameter d_- determines, where the orientational order crosses over from power law to exponential behavior in the two-phase regime. The best agreement between $\overline{\rho}_\alpha$ and experimental data for the mixture 2NC was found with $\xi^s_{o+}=0.42$ nm, $M_D=-15.1$, and $d_-=0.5$ (heavy solid line).

This model for $\alpha_2(z)$ also provides a good description for the 4NC critical mixture [Fig. 1(b)] with the same value of $d_-(=0.5)$ while $\xi^s_{o+}=0.35$ nm and $M_D=-6.2$. Hence, the results for both 2NC and 4NC imply that the dipoles are preferentially oriented parallel to the interface $(M_D<0)$ and are repelled from the interface $(\xi^s_{o+}>\xi^b_{o+})$, in agreement with the simple electrostatic considerations [Eq. (1)]. Figure 3 exhibits the variation in orientational order α_2 with $x=z/\xi$ for $t=0.01$ and 0.001, where α_2 is very sharply peaked at the surface, indicating that the dipoles are strongly oriented parallel to the surface the closer these dipoles are to $x=0$. However, one must additionally keep in mind that dipoles are desorbed from the surface so that there are fewer and fewer dipoles the closer one is to the surface. In prior work [10] we have shown that the quantity $\hat{v}(z)=[1-v(z)]\alpha_2(z)/4\pi$ [which incorporates the effects of both $\alpha_2(z)$ and $v(z)$] provides a good description of earlier com-

puter simulations [18] for the orientation of a highly dipolar *pure* fluid far from its critical point.

VI. DISCUSSION

In this publication we have used the experimental technique of ellipsometry to examine the orientational order that occurs at the liquid-vapor surface of two highly dipolar + nonpolar critical binary liquid mixtures. For the systems considered, the dipolar component is desorbed from the surface by the short-ranged (surface tension) interactions but also repelled from the surface by the long-ranged dipole–image-dipole interaction [Eq. (1)], where the dipoles in the vicinity of the surface are oriented preferentially parallel to the interface. More extensive calculations provide confirmation of this simple electrostatic picture. In particular, the local volume fraction $v(z)$ of the nonpolar *adsorbed* component is described by Eqs. (2)–(6) while the local orientational order for dipolar molecules $\alpha(z,\theta)$ [Eq. (9)] with z dependence $\alpha_2(z)$ is described by Eqs. (17) and (18). In these equations there are 4 adjustable parameters ξ_{o+}, M_D, d_-, and ξ_{nc}. Each of these parameters has a differing influence on the ellipticity $\overline{\rho}$. The noncritical correlation length ξ_{nc} [Eq. (30)] merely adds a constant background to $\overline{\rho}$, for all reduced temperatures t, and cannot change the shape of the $\overline{\rho}$ curve. The correlation length amplitude ξ_{o+} influences both the peak reduced temperature $t_{\rm peak}$ (in the one-phase region) and the ellipticity amplitude $\Delta\overline{\rho}$; as ξ_{o+} increases both $t_{\rm peak}$ and $\Delta\overline{\rho}$ increase. For simplicity we assume that ξ_{o+} is the same for both the local volume fraction and the local orientational order. The orientational order amplitude M_D primarily decreases (increases) $\Delta\overline{\rho}$ for negative (positive) value, relative to the behavior in the absence of orientational order (i.e., $M_D=0$); M_D has marginal influence on $t_{\rm peak}$. Finally, the orientational order crossover parameter d_- determines where the system crosses over from power law to exponential behavior with increasing dimensionless distance z/ξ in the two-phase region. For the dipolar + nonpolar systems, 2-nitroanisole + cyclohexane (2NC) and 4-nitroanisole + cyclohexane (4NC), we found that the best fit between the $\alpha_2(z)$ model and experimental data (Figs. 1(a) and 1(b) heavy solid line) occurred for $d_-=0.5$ for both systems, which implies that $\alpha_2(z)$ is described by a *universal* surface scaling function as expected from scaling theory. Different systems give rise to different surface behavior through the two system dependent parameters ξ_{o+} and M_D, which are expected to be functions of the reduced dipole moment p^*. For both 2NC and 4NC, the optimal fit (Fig. 1 and Table II) occurred for (i) $\xi_{o+}\equiv\xi^s_{o+}$, a surface correlation length amplitude where $\xi^s_{o+}>\xi^b_{o+}$, the mixture's bulk value, (i.e., the dipoles are repelled from the interface by the interaction with their image dipoles) and (ii) an orientational amplitude $M_D<0$, implying that the dipoles are oriented preferentially parallel to the interface [44]. These results agree with the simple electrostatic considerations of Eq. (1).

The two system dependent parameters, $\xi^s_{o+}(p^*)$ and $|M_D(p^*)|$, are expected to be *monotonically increasing* functions of the reduced dipole moment p^*, where for $p^*=0$, $\xi^s_{o+}(0)=\xi^b_{o+}$ and $M_D(0)=0$. Measurements of the gaseous dipole moment indicate that $p^*(2\mathrm{NC})\lesssim p^*(4\mathrm{NC})\sim 2$ (Table III). By contrast, the results in this paper indicate that $p^*(2\mathrm{NC})>p^*(4\mathrm{NC})$, because ξ^s_{o+} and $|M_D|$ for 2NC are significantly larger than the values for 4NC. How can this be? A likely solution to this dilemma is that in liquids or liquid mixtures, two or more nitroanisole molecules self-associate and it is this self-associated cluster with an ''effective'' dipole moment p^*_e which orients at the liquid-vapor interface. Nitroanisole, with chemical formula $C_7H_7NO_3$, consists of a benzene ring, where the NO_2 group is either adjacent to (for 2N) or diametrically opposite to (for 4N) the methoxy group -C-CH_3. Thus, 2-nitroanisole is likely to self-associate rather differently compared with 4-nitroanisole, in the liquid phase; which in turn will give rise to differing effective dipole moments. The Kirkwood structure parameter g provides a measure of the correlation and clustering of molecules in the liquid phase. For $g\simeq 1$ adjacent molecules are uncorrelated, while $g\gg 1$ provides evidence that molecules are correlated. The Kirkwood structure parameter can be estimated from [45]

$$g=\frac{9k_BT}{4\pi kN_o p^2}\frac{[\varepsilon_S-\varepsilon][2\varepsilon_S+\varepsilon]}{\varepsilon_S(\varepsilon+2)^2}\tilde{V}, \tag{33}$$

where k_BT is the thermal energy, N_o is Avogradro's number, ε_S is the static dielectric constant, and $\tilde{V}$ is the molar volume. Surprisingly $g\simeq 1$ (Table III), indicating that the nitroanisole molecules are uncorrelated in solution. Hence, at this time, we do not have an explanation for why our data indicates that $p^*_e(2\mathrm{NC})>p^*_e(4\mathrm{NC})$. An alternative method for characterizing the p^*_e dependence of $\xi^s_{o+}(p^*_e)$ and $M_D(p^*_e)$ (without having to measure p^*_e) is to plot ξ^s_{o+}/ξ^b_{o+} as a function of $-M_D$, where p^*_e is a parametric parameter. The point (1,0) corresponds to a nonpolar mixture. A continuous monotonically increasing curve should pass through the points (1,0), 2NC, and 4NC, as schematically depicted in Fig. 4. Obviously more experimental points are required to accurately define this curve, which we suspect is *universal* and therefore should provide a strong test of any future theory.

These experiments on dipole orientational order at the *noncritical* liquid-vapor surface, as well as, the earlier experiments on dipole orientational order at the *critical* liquid-liquid surface, raise an interesting question. Why are the functional forms for $\alpha_2(z)$ for the critical [Eq. (10)] and noncritical [Eq. (17)] interfaces so different? One possibility is that this is just the way nature is for the critical and noncritical interfaces, after minimization of the surface free energy with respect to the local volume fraction and the local orientational order. A more provocative possibility is that Eq. (10), applicable for the critical interface, is valid in the limit of weak dipole–image-dipole interactions [the difference in the static dielectric constants between the two phases $\Delta\varepsilon_S\to 0$ as $T\to T_c$], while Eq. (17), applicable for the noncritical interface, is valid in the limit of strong dipole–image-dipole interactions [$\Delta\varepsilon_S$ is always large].

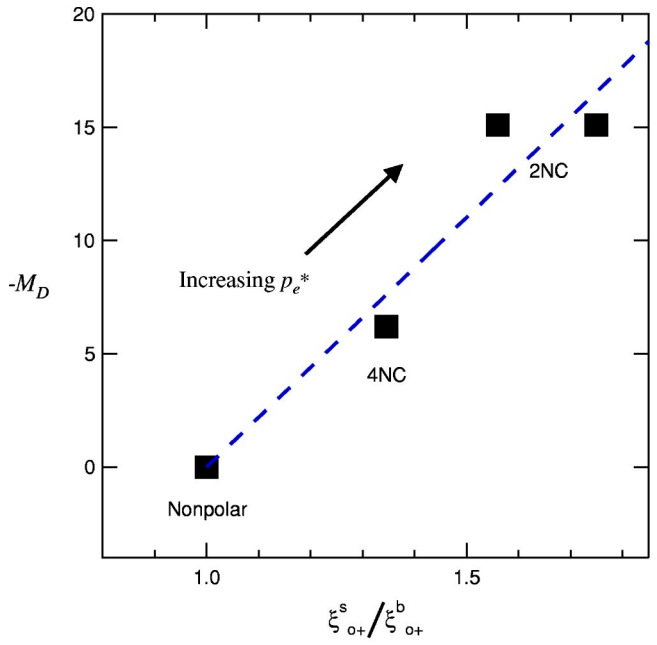

FIG. 4. Plot of $-M_D$ as a function of ξ^s_{o+}/ξ^b_{o+} for nonpolar, 4NC and 2NC mixtures. The direction of increasing effective dipole moment p_e^* is indicated, the dashed line is a guide to the eye, while the two 2NC symbols originate from the two ξ^b_{o+} values in Table IV.

We view this work as just the beginning of an extensive investigation into the physical origins of surface orientational order at liquid-vapor or liquid-solid surfaces. As discussed in the introduction, there is a plethora of different classes of surface orientational order that have not been investigated either experimentally or theoretically. In this paper we have only studied the behavior of dipoles at liquid-vapor interfaces in class Bb where both the short- and long-ranged forces on the dipoles are repulsive. From simple electrostatic considerations [Eq. (1)] one expects differing behavior in class Aa, where both the short- and long-ranged forces on the dipole are attractive, as well as in classes Ab and Ba where the short- and long-ranged forces oppose each other. In each of these classes, the strength of the dipole–image-dipole interaction for liquid-solid surfaces could be tuned by appropriate selection of the solid dielectric constant relative to the liquid value.

ACKNOWLEDGMENTS

We would like to thank S. Dietrich and co-workers for detailed discussions. This research work has been supported by the National Science Foundation through Grant No. DMR-0097119.

APPENDIX: ELLIPTICITY CALCULATION

In Sec. IV C, the local volume fraction $v(z)$ and local orientational order $\alpha_2(z)$ at depth z were related to the local dielectric constants parallel $[\varepsilon_{\|}(z)]$ and perpendicular $[\varepsilon_{\perp}(z)]$ to the interface. In this Appendix, we provide a general description of how to numerically calculate the ellipticity $\overline{\rho}$ from this dielectric model of the interface. The algorithm that we follow is based upon a 4×4 matrix method for anisotropic media [40,41,46], that has been suitably modified for our specific purposes. Most previous calculations have been applied to describe the properties of elliptically polarized light reflected from solid crystalline monolayers (or multilayers), which were at a specified, but arbitrary, orientation relative to the optical plane of incidence. These calculations are complex and possess far greater generality than required when considering reflection from an anisotropic *liquid* surface. For liquids, with z normal to the liquid-vapor surface and an xz plane of incidence, molecules are free to rotate in the xy plane. In this case, it is only necessary to consider a locally anisotropic dielectric interface with principal axes parallel to the xyz axes with a local diagonal dielectric tensor

$$\varepsilon(z)=\begin{bmatrix}\varepsilon_x(z) & 0 & 0\\ 0 & \varepsilon_y(z) & 0\\ 0 & 0 & \varepsilon_z(z)\end{bmatrix}, \tag{A1}$$

where, in the bulk liquid $(z\rightarrow\infty)$ and vapor $(z\rightarrow-\infty)$ phases, $\varepsilon(z)$ is isotropic and constant. In the absence of any sources, Maxwell's equations are

$$\nabla\times\mathbf{E}=-\frac{\partial\mathbf{B}}{\partial t},\quad \nabla\times\mathbf{H}=\frac{\partial\mathbf{D}}{\partial t}, \tag{A2}$$

where **H** and **E** denote the magnetic and electric fields, respectively. For dielectric media, the electric displacement **D** and magnetic induction **B** are given by

$$\mathbf{D}=\varepsilon_o\varepsilon(z)\mathbf{E},\quad \mathbf{B}=\mu_o\mathbf{H}, \tag{A3}$$

where ε_o and μ_o are, respectively, the dielectric permittivity and magnetic permeability in vacuum with speed of light $c=1/\sqrt{\varepsilon_o\mu_o}$.

For a monochromatic plane wave of frequency ω_o, incident wave vector $\mathbf{k}_i$, at incident angle θ_i to the z axis, Maxwell's equations can be further simplified to

$$\frac{\partial\mathbf{\Psi}}{\partial z}=ik_o\mathbf{K}\mathbf{\Psi}, \tag{A4}$$

where

$$\mathbf{\Psi}=\begin{bmatrix}\sqrt{\varepsilon_o}E_x\\ \sqrt{\varepsilon_o}E_y\\ \sqrt{\mu_o}H_x\\ \sqrt{\mu_o}H_y\end{bmatrix}, \tag{A5}$$

$$\mathbf{K}=\begin{bmatrix} 0 & 0 & 0 & 1-\left(\frac{k_x}{k_o}\right)^2\frac{1}{\varepsilon_x} \\ 0 & 0 & -1 & 0 \\ 0 & \left(\frac{k_x}{k_o}\right)^2-\varepsilon_y & 0 & 0 \\ \varepsilon_x & 0 & 0 & 0 \end{bmatrix} \tag{A6}$$

with $k_o=\omega_o/c$ and $k_x=\mathbf{k}_i\cdot\hat{\mathbf{x}}$. Thus, the field vector at Z can be related to the field vector at $z=0$ via

$$\mathbf{\Psi}(Z)=\mathbf{M}\mathbf{\Psi}(0), \tag{A7}$$

where the characteristic matrix is

$$\mathbf{M}=\exp\left\{ ik_o\int_0^Z \mathbf{K}dz\right\}. \tag{A8}$$

For N sufficiently thin layers ($\ll\lambda$), where $\mathbf{K}$ does not vary significantly within each layer, then the characteristic matrix can be expressed as

$$\begin{aligned}\mathbf{M}&=\exp\left\{ ik_o\left(\int_0^{z_1}\mathbf{K}dz+\int_{z_1}^{z_2}\mathbf{K}dz+\cdots+\int_{z_{N-1}}^{Z}\mathbf{K}dz\right)\right\} \\ &\simeq\left(\mathbf{I}+ik_o\int_0^{z_1}\mathbf{K}dz\right) \\ &\quad\times\left(\mathbf{I}+ik_o\int_{z_1}^{z_2}\mathbf{K}dz\right)\cdots\left(\mathbf{I}+ik_o\int_{z_{N-1}}^{Z}\mathbf{K}dz\right) \\ &=m_1m_2\cdots m_{N-1}m_N \\ &=\prod_{j=1}^{N} m_j,\end{aligned} \tag{A9}$$

where, to leading order, the submatrix $\mathbf{m}_j$ in the jth layer is given by

$$\mathbf{m}_j=\begin{bmatrix} 1 & 0 & 0 & ik_o\int\left(1-\alpha^2\frac{1}{\varepsilon_z}\right)dz \\ 0 & 1 & ik_o\int(-1)dz & 0 \\ 0 & ik_o\int(\alpha^2-\varepsilon_y)dz & 1 & 0 \\ ik_o\int\varepsilon_x dz & 0 & 0 & 1 \end{bmatrix}, \tag{A10}$$

the symbol $\int\equiv\int_{z_{j-1}}^{z_j}$, and Snell's factor $\alpha\equiv(\mathbf{k}_i\cdot\hat{\mathbf{x}})/k_o=\sin\theta_i$. In the numerical calculation, the matrix multiplication [Eq. (A9)] forms the most time consuming step. The accuracy and efficiency of this calculation can be considerably improved by considering a linear dielectric $\varepsilon_j=a_jz+b_j$ within the jth layer [39], where

$$a_j=\frac{\varepsilon_j-\varepsilon_{j-1}}{z_j-z_{j-1}} \tag{A11}$$

and

$$b_j=\frac{\varepsilon_{j-1}z_j-\varepsilon_jz_{j-1}}{z_j-z_{j-1}}. \tag{A12}$$

The integrals within $\mathbf{m}_j$ [Eq. (A10)] can therefore be explicitly evaluated via

$$\int_{z_{j-1}}^{z_j}\frac{1}{\varepsilon_j}dz\simeq\left[\frac{1}{a_j}\ln(a_jz+b_j)\right]_{z=z_{j-1}}^{z=z_j}, \tag{A13}$$

$$\int_{z_{j-1}}^{z_j}\varepsilon_j dz\simeq\left[\frac{a_jz^2}{2}+b_jz\right]_{z=z_{j-1}}^{z=z_j}, \tag{A14}$$

and

$$\int_{z_{j-1}}^{z_j}dz\simeq[z]_{z=z_{j-1}}^{z=z_j}. \tag{A15}$$

The numerical solution now converges remarkably quickly as a function of the number of layers N. The electric $\mathbf{E}$ and magnetic $\mathbf{H}$ fields within the isotropic bulk media at 0 and Z, on either side of the surface, can be reexpressed in terms of the incident, reflected, and transmitted electric fields $\mathbf{E}^i$, $\mathbf{E}^r$, and $\mathbf{E}^t$ [47], respectively, which transforms Eq. (A7) into

$$\begin{bmatrix} E_x^t \\ E_y^t \\ -n\cos\theta_tE_y^t \\ nE_x^t/\cos\theta_t \end{bmatrix}=\mathbf{M}\begin{bmatrix} (E_x^i+E_x^r) \\ (E_y^i+E_y^r) \\ -\cos\theta_i(E_y^i-E_y^r) \\ (E_x^i-E_x^r)/\cos\theta_i \end{bmatrix}, \tag{A16}$$

where $n(=\sqrt{\varepsilon_l})$ is the refractive index of the liquid phase and θ_t is the angle of transmittance. If the transmitted electric field $\mathbf{E}^t$ is eliminated from this sequence of equations and the electric fields are projected onto the p and s polarization axes using $E_x^i = E_p^i \cos\theta_i$ and $E_x^r = E_p^r \cos\theta_i = -E_p^r \cos\theta_i$ then

$$\begin{bmatrix} E_p^r \\ \\ E_s^r \end{bmatrix} = \begin{bmatrix} r_p & 0 \\ 0 & r_s \end{bmatrix} \begin{bmatrix} E_p^i \\ \\ E_s^i \end{bmatrix}, \tag{A17}$$

where

$$r_p = \frac{[M_{11} - M_{41}(\cos\theta_t)/n]\cos\theta_i + [M_{14} - M_{44}(\cos\theta_t)/n]}{[M_{11} - M_{41}(\cos\theta_t)/n]\cos\theta_i - [M_{14} - M_{44}(\cos\theta_t)/n]}, \tag{A18}$$

$$r_s = \frac{[M_{33} + M_{23} n \cos\theta_t]\cos\theta_i - [M_{32} + M_{22} n \cos\theta_t]}{[M_{33} + M_{23} n \cos\theta_t]\cos\theta_i + [M_{32} + M_{22} n \cos\theta_t]}, \tag{A19}$$

and M_{ij} is the ijth element of the characteristic matrix $\mathbf{M}$ [Eq. (A8)]. After setting $\varepsilon_\parallel(z) = \varepsilon_x(z) = \varepsilon_y(z)$ and $\varepsilon_\perp(z) = \varepsilon_z(z)$, Eqs. (A18) and (A19) can be used to determine the Brewster angle θ_B from $\mathrm{Re}(r_p/r_s)|_{\theta_B} = 0$ [Eq. (21)] and the ellipticity from $\overline{\rho} = \mathrm{Im}(r_p/r_s)|_{\theta_B}$ [Eq. (20)]. In practice, the total width of the interface was taken as $Z \simeq 20\xi$, where $\varepsilon(Z)$ differed from the bulk dielectric constant by less than 10^{-9} and the number of layers $N = 2000$ ensured that $\overline{\rho}$ was accurate to better than 1% for all reduced temperatures.

For sufficiently thin interfaces compared with the wavelength of light λ, a single layer of the characteristic matrix is sufficient to determine $\overline{\rho}$, namely, $\mathbf{M} \simeq \mathbf{m}_1$. The modified Drude equation [Eq. (22)], with $\varepsilon_x = \varepsilon_y = \varepsilon_\parallel$ and $\varepsilon_z = \varepsilon_\perp$, can then be derived from this approximation.

[1] M. E. Fisher and P.-G. de Gennes, C. R. Seances Acad. Sci., Ser. B **287**, 207 (1978).
[2] A. W. Adamson, *Physical Chemistry of Surfaces*, 4th ed. (Wiley, New York, 1982).
[3] H. W. Diehl, Int. J. Mod. Phys. B **11**, 3503 (1997).
[4] U. Ritschel and P. Czerner, Phys. Rev. Lett. **77**, 3645 (1996).
[5] J.-H. J. Cho and B. M. Law, Phys. Rev. Lett. **86**, 2070 (2001).
[6] K. E. Gubbins, in *Fluid Interfacial Phenomena*, edited by C. A. Croxton (Wiley, New York, 1986).
[7] B. Groh and S. Dietrich, in *New Approaches to Problems in Liquid State Theory*, edited by C. Caccamo, J. P. Hansen, and G. Stell (Kluwer, Dordrecht, 1999).
[8] J. D. Jackson, *Classical Electrodynamics*, 2nd ed. (Wiley, New York, 1975).
[9] P. Frodl and S. Dietrich, Phys. Rev. E **48**, 3741 (1993).
[10] J.-H. J. Cho and B. M. Law, Phys. Rev. Lett. **89**, 146101 (2002).
[11] J.-H. J. Cho, B. M. Law, and K. Gray, J. Chem. Phys. **116**, 3058 (2002).
[12] J. H. Carpenter, J.-H. J. Cho, and B. M. Law, Phys. Rev. E **61**, 532 (2000).
[13] In determining the parameters in Eq. (4), two of the fourteen parameters were adjustable in order to improve the agreement between theory and experiment; the remaining twelve parameters were determined by theoretical or experimental constraints [12].
[14] H. B. Tarko and M. E. Fisher, Phys. Rev. Lett. **31**, 926 (1973); A. J. Liu and M. E. Fisher, Physica A **156**, 35 (1989); C. Ruge, P. Zhu, and F. Wagner, *ibid.* **209**, 431 (1994).
[15] J. H. Carpenter, B. M. Law, and D. S. P. Smith, Phys. Rev. E **59**, 5655 (1999).
[16] A. J. Liu and M. E. Fisher, Phys. Rev. A **40**, 7202 (1989).
[17] T. J. Sluckin, Mol. Phys. **43**, 817 (1981); **47**, 267 (1982).
[18] J. Eggebrecht, K. E. Gubbins, and S. M. Thompson, J. Chem. Phys. **86**, 2286 (1987); J. Eggebrecht, S. M. Thompson, and K. E. Gubbins, *ibid.* **86**, 2299 (1987).
[19] E. Chacón, P. Tarazona, and G. Navascués, J. Chem. Phys. **79**, 4426 (1983); P. I. Teixerira and M. M. Telo da Gama, J. Phys.: Condens. Matter **3**, 111 (1991); M. Iwamoto, A. Sugimura, and O.-Y. Zhong-can, Phys. Rev. E **54**, 6537 (1996).
[20] B. Yang, D. E. Sullivan, B. Tjipto-Margo, and C. G. Gray, J. Phys.: Condens. Matter **3**, F109 (1991).
[21] Y. R. Shen, *The Principles of Nonlinear Optics* (Wiley, New York, 1984).
[22] H. Hsiung, Th. Rasing, and Y. R. Shen, Phys. Rev. Lett. **57**, 3065 (1986); W. Chen, L. J. Martinez-Miranda, H. Hsiung, and Y. R. Shen, *ibid.* **62**, 1860 (1989).
[23] B. M. Ocko, A. Braslau, P. S. Pershan, J. Als-Nielsen, and M. Deutsch, Phys. Rev. Lett. **57**, 94 (1986); B. M. Ocko, *ibid.* **64**, 2160 (1990).
[24] P. I. C. Teixeira, B. S. Almeida, M. M. Telo da Gama, J. A. Rueda, and R. G. Rubio, J. Phys. Chem. **96**, 8488 (1992).
[25] A. Mukhopadhyay, C. L. Caylor, and B. M. Law, Phys. Rev. E **61**, R1036 (2000).
[26] A. Mukhopadhyay and B. M. Law, Phys. Rev. E **63**, 011507 (2000).
[27] S. Fisk and B. Widom, J. Chem. Phys. **50**, 3219 (1969).
[28] C. L. Caylor, B. M. Law, P. Senanayake, V. L. Kuzmin, V. P. Romanov, and S. Wiegand, Phys. Rev. E **56**, 4441 (1997).
[29] B. Widom, J. Phys. Chem. **100**, 13 190 (1996).
[30] L. W. DaMore and D. T. Jacobs, J. Chem. Phys. **97**, 464 (1992).
[31] D. Beaglehole, in *Fluid Interfacial Phenomena*, edited by C. A. Croxton (Wiley, New York, 1986).
[32] B. M. Law, Prog. Surf. Sci. **66**, 159 (2001).
[33] D. Beaglehole, Physica B & C **100**, 163 (1980).
[34] J.-H. Cho, Ph.D. dissertation, Kansas State University, 2002 (unpublished).
[35] D. S. P. Smith and B. M. Law, Phys. Rev. E **52**, 580 (1995); **54**, 2727 (1996).

[36] F. Abelès, Ann. Phys. (Paris) **5**, 596 (1950).
[37] J. Lekner, *Theory of Reflection* (Martinus Nijhoff, Dordrecht, 1987).
[38] M. Born and E. Wolf, *Principle of Optics* (Pergamon, Oxford, 1980), Sec. 1.6.
[39] B. M. Law and D. Beaglehole, J. Phys. D **14**, 115 (1981).
[40] D. W. Berreman, J. Opt. Soc. Am. **63**, 1374 (1973).
[41] Y. Tabe and H. Yokoyama, Langmuir **11**, 699 (1995).
[42] J. N. Israelachvili, *Intermolecular and Surface Forces*, 2nd ed. (Academic, London, 1992).
[43] R. F. Kayser, Phys. Rev. B **34**, 3254 (1986).
[44] Note, as we have assumed for simplicity that ξ^{s}_{o+} is the same for both $v(z)$ and $\alpha_2(z)$, the local volume fraction and the local orientational order both decay over identical length scales. This length scale considerably exceeds the length scale governed by bulk correlations.
[45] W. R. Fawcett, Mol. Phys. **86**, 715 (1995).
[46] P. J. Lin-Chung and S. Teitler, J. Opt. Soc. Am. A **1**, 703 (1984).
[47] E. Hecht, *Optics*, 4th ed. (Addison-Wesley, San Francisco, 2002).
[48] H. A . Stuart, *Molekülstruktur* (Springer-Verlag, Berlin, 1934).
[49] L. G. Groves and S. Sugden, J. Chem. Soc. **1937**, 1782 (1937).